

## Amide Proton Transfer (APT) imaging of uterine tumors: a preliminary clinical study

Yukihisa Takayama<sup>1</sup>, Akihiro Nishie<sup>2</sup>, Osamu Togao<sup>1</sup>, Yoshiki Asayama<sup>2</sup>, Yasuhiro Ushijima<sup>2</sup>, Nobuhiro Fujita<sup>2</sup>, Takashi Yoshiura<sup>2</sup>, Makoto Obara<sup>3</sup>, Jochen Keupp<sup>4</sup>, and Hiroshi Honda<sup>2</sup>

<sup>1</sup>Department of Molecular Imaging and Diagnosis, Graduate School of Medical Sciences, Kyushu University, Fukuoka, Fukuoka, Japan, <sup>2</sup>Department of Clinical Radiology, Graduate School of Medical Sciences, Kyushu University, Fukuoka, Fukuoka, Japan, <sup>3</sup>Philips Electronics Japan, Tokyo, Tokyo, Japan, <sup>4</sup>Philips Technologie GmbH Forschungslaboratorien, Hamburg, Germany

### Introduction

Amide Proton Transfer (APT) may provide a powerful new tool for MR molecular imaging. APT imaging is based on the chemical exchange between bulk water protons and labile solute protons, such as those bearing NH- and OH- groups [1]. Recently, CEST imaging based on parallel radiofrequency transmission was demonstrated and the utility of APT imaging of brain tumor has been reported [2,3]. However, there has been no report about APT imaging of uterine tumors. The purpose of this study was to investigate the clinical feasibility of APT imaging for uterine tumors.

### Materials and Methods

Twenty-four patients with uterine tumors (5 endometrial carcinomas and 19 squamous cell carcinomas) were included in this study. In addition to conventional MR imaging, such as T2WI and DWI, APT imaging was scanned on a 3T clinical scanner (Achieva TX 3.0T, Philips Healthcare, NL) using a 32-channel SENSE Torso/Cardiac coil for signal reception and 2-channel parallel transmission via the body coil. Acquisition software was modified to alternate the operation of the two transmission channels during the radiofrequency saturation pulse and to allow a special radiofrequency shimming for the saturation homogeneity of the alternated pulse (identical mean B1 level per channel) [3]. Saturation pulse-trains: 50ms sinc-gaussian elements,  $B_1=2.0 \mu\text{T}$ . 2D fast spin-echo sequences with driven equilibrium refocusing were used [3]. The imaging parameters were as follows:  $T_{\text{sat}}=0.5 \text{ s}$ ,  $\text{TR}/\text{TE}=5000/6 \text{ ms}$ ,  $\text{FOV}=230 \text{ mm}^2$ ,  $\text{matrix}=168^2$ ,  $\text{resolution}=1.8 \times 1.8 \times 5 \text{ mm}^3$ , 25 saturation frequency offsets  $S[\omega]$ ,  $\omega = -6.0$  to  $+6.0 \text{ ppm}$  (step 0.5 ppm) and  $S_0$  ( $\omega = -160 \text{ ppm}$ ), affording 2 minutes scanning time.  $\delta B_0$  maps for off-resonance correction were acquired separately (identical geometry, 2D GRE,  $\Delta\text{TE}=1 \text{ ms}$ ,  $\text{TR}/\text{TE}=15\text{ms}/8\text{ms}$ , 16 averages, 33 sec) while carefully fixing the resonance frequency reference and shimming as well as using low gradient strength to minimize B0 eddy current effects. MTR asymmetry ( $\text{MTR}_{\text{asym}}$ ) was defined as:  $\text{MTR}_{\text{asym}} = \{S_{\text{sat}}(-\omega) - S_{\text{sat}}(+\omega)\}/S_0$ , as defined above. A map of the APT ratio (APTR) was defined as  $\text{MTR}_{\text{asym}}$  at the saturation offset of 3.5ppm. Region-of-interests were carefully placed in the entire area of uterine tumors to measure  $\text{MTR}_{\text{asym}}$  and APTR.

### Results

Figure 1 shows the spectra of  $\text{MTR}_{\text{asym}}$  in both tumor types. The spectra of  $\text{MTR}_{\text{asym}}$  of endometrial carcinoma were significantly higher than those of squamous cell carcinoma at the frequency offset from 2.2 ppm to 3.7 ppm and from 4.8 ppm to 5.1 ppm ( $p < 0.05$ , Mann-Whitney  $U$  test). However, there were overlaps between the two at the frequencies of less than 2.2 ppm, from 3.7 ppm to 4.8 ppm and more than 5.1 ppm. Table 1 shows average and standard deviation (SD) of APTR in both tumor types. APTRs of endometrial carcinoma were significantly higher than those of squamous cell carcinoma ( $p < 0.05$ , Mann-Whitney  $U$  test). Figure 2 demonstrates representative cases of T2WI, DWI and APTR map of endometrial and squamous cell carcinomas. APTR map shows that APTR of endometrial carcinoma is higher than that of squamous cell carcinoma.

### Discussion and Conclusion

APT imaging showed that  $\text{MTR}_{\text{asym}}$  and APTR of endometrial carcinoma were higher than those of squamous cell carcinoma. It was speculated that higher  $\text{MTR}_{\text{asym}}$  and APTR of endometrial carcinoma might be related to the characteristic as a malignant tumor originating in glandular tissue. T2WI and DWI were useful for the evaluation tumor site, tumor size, and local extension of tumors. In addition, DWI can provide information about tumor cellularity. Meanwhile, APT imaging also provide molecular information of tumors, including histological characteristics, by taking a different approach as compared to DWI or contrast-enhanced MRI. Although further investigation is necessary, we suggest that APT imaging is feasible as a new diagnostic tool in clinical practice for the differential diagnosis of uterine tumors.

### References

- [1] Zhou J, et al. Progr NMR Spectr 48:109-136 (2006).  
 [2] Togao O, et al. Proceedings of the annual meeting of ISMRM 20:744 (2012).  
 [3] Keupp J, et al. Proceedings of the annual meeting of ISMRM 19:710 (2011).

**Table 1. Average and SD of APTR in both tumor types**

Tumor	APTR [%] average $\pm$ SD (range)	Mann-Whitney $U$ test
Endometrial carcinoma (n=5)	5.7 $\pm$ 2.8 (3.3-10.4)	] $p < 0.05$
Squamous cell carcinoma (n=19)	3.0 $\pm$ 1.2 (1.4-5.6)	

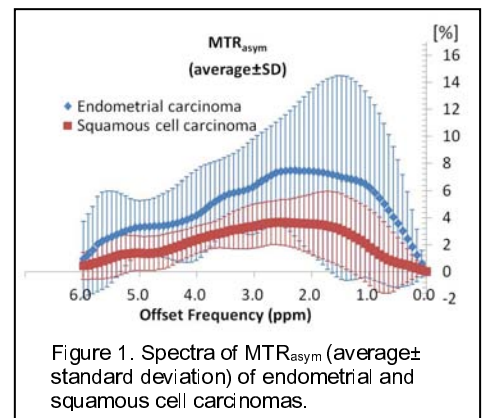


Figure 1. Spectra of  $\text{MTR}_{\text{asym}}$  (average $\pm$  standard deviation) of endometrial and squamous cell carcinomas.

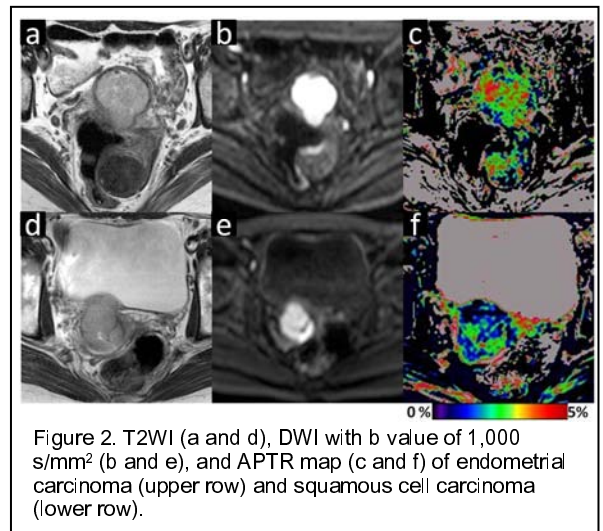


Figure 2. T2WI (a and d), DWI with b value of 1,000  $\text{s}/\text{mm}^2$  (b and e), and APTR map (c and f) of endometrial carcinoma (upper row) and squamous cell carcinoma (lower row).